Development of A New Geomaterial Damping Block with Suitable Characteristics for Use in Planting Basemats

Y. Ikeda
Taisei Corporation, Tokyo, Japan

Y. Shimomura & N. Sako
Nihon University Junior College, Chiba, Japan

T. Fujikawa
Graduate Student, College of Science & Technology, Nihon University, Chiba, Japan

M. Kawamura
College of Industrial Technology, Nihon University, Chiba, Japan

SUMMARY
A new soil material that is made of industrial wastes and construction by-products has been developed by authors. In this paper, the dynamic characteristics of the new geomaterial damping block for planting (GDBP) that is composed of the above soil material that contains wood chips for water retention and has high attenuation performance have been investigated. Preliminary seismic calculations of a building assumed to be constructed at weak and soft soil condition sites have been also carried out taking into account GDBP as seismic isolation and plant cultivation materials.

Keywords: Damping performance, Geomaterial damping block, Construction by-products, Planting basemat

1. INTRODUCTION

Many of mid-rise or high-rise buildings have recently been constructed on weak soil sites where are coast zones or landfills of large urban areas without effective measures against large earthquakes. Although buildings equipped with isolation devices are one of the seismic countermeasures, a large cost burden has been imposed to the owners and this has prevented wide spread of these building constructions.

In this paper, a new soil material using industrial wastes and by-products of constructions has been proposed (Fujikawa *et al.*, 2011). This new soil material has high attenuation performance and planting capability. The dynamic characteristics of this geomaterial damping block for planting (GDBP) that contains wood chips for water retention has been investigated by dynamic triaxial compression tests in the laboratory. In order to grasp and validate the dynamic behaviour of GDBP for seismic response of a structure, preliminary seismic calculations have been conducted. It is assumed that GDBP is backfilled in circumference of the basemat in order to utilize as plant cultivation areas and parking lots. In some calculations, high rigidity damping material (HRDM) that has already been reported (Hirota *et al.*, 1993, Sako *et al.*, 2010) is used as a supporting material for GDBP. HRDM is a composite of crushed stones, waste tire chips and asphalt. In these analyses, modelling of basemat, soil, GDBP and HRDM is performed using the 3D axial symmetry FE models.

Currently, after one year from the 2011 off the Pacific coast of Tohoku Earthquake, rubble of the earthquake has not been segregated and has not been also accumulated on temporary storage areas. It is believed that dealing effectively and rapidly with the huge rubble with reduction of the effects on the environment is the most priority role for emergency restoration of the earthquake. Concrete rubble that is not needed radiation decontamination will be used as the recycled fine powder of GDBP. In addition, the asphalt roadbed rubble and waste wood will be utilized for recycled asphalt and wood chips of GDBP, respectively. We clarify that GDBP can be used as the material that increases the soil

height of disaster areas that were sunken or flooded by tsunamis and earthquakes. Based on the one-dimensional wave propagation analysis, the aseismic effectiveness of GDBP that is adopted as the height increasing material for the damaged soil areas of the afflicted district is investigated.

2. OUTLINE OF DYNAMIC TRIAXIAL COMPRESSION TESTS

2.1 Used materials for tests

Specimens of GDBP that were adopted for the tests were developed using materials shown in Table 2.1. In order to possess the planting capability of GDBP, wood-chips shall be used as an admixture surely. In this paper, wood-chips, recycled fine powder, granulated blast furnace slag, asphalt emulsion and water are abbreviated respectively as WC, RF, BS, EA and WT. Photos of each material are illustrated in Figure 2.1.

2.2 Development procedure of specimens

Quantity of each admixture designated in Table 2.2 was mixed in a container and stirred in one minute. Qualities of EA and WT designated in Table 2.2 were then mixed in another container and stirred in one minute. Two mixtures were combined and stirred in three minutes, and then a pasty blended material was generated. The pasty blended material was poured in the steel mold (diameter = 50mm and height = 100mm) in which the remover was sprayed inside, and then GDBP was generated. Productions of all specimens were performed per three layers and compaction of ten times per each layer was carried out. Curing of the specimens was done in air, and the material age for all specimens was assumed to be 28 days.

Table 2.1. Materials used

Material		Description	Role
Wood-chip	WC	Crushed timber with an aspect ratio of 4 to 25 and max. length of 40mm	Main admixture
Recycled fine powder	RF	Crushed concrete with a diameter less than 5mm	Admixture
Blast furnace slag	BS	Glassy slag made as a by-product other than iron in the process of purifying the iron in the blast furnace	Admixture
Asphalt emulsion	EA	A nonionic emulsion solidifies at normal temperatures	Binder
Water	WT	Tap water	Binder

Table 2.2. Admixture for each specimen

Specimen	Admixture (WC/RF/BS)	Binder (EA/WT)	Curing period	Layer compaction
A	0.67/0.33/0	0.85/0.15	28days	3 layers (10 time compactions for each layer)
B	0.33/0.67/0			
C	0.67/0.17/0.17			
D	0.33/0.33/0.33			

(a) Wood-chip   (b) Recycled fine powder   (c) Asphalt emulsion   (d) Specimen example

Figure 2.1. Main materials and specimen example

2.3 Test methods

Cyclic triaxial tests were conducted in accordance with the reference book (the Japanese Geotechnical Society, 2009). Tests were carried out with testing machines of the cyclic triaxial test. Displacement gauges for large displacement (range of measurement: 1/100 – 200mm) and microdisplacement (range of measurement: 1/1000 - 1mm) were used and load cell whose capacity is 2kN was used for load measurements. The maximum depth for bottom surface of GDBP and confined pressure were assumed to be approximately 5m and 50kPa, respectively. As GDBP is assumed not to be used deeper than ground water level, the specimens were tested on condition of undersaturation. The confined pressures used in the triaxial compression tests were the same as these in the cyclic triaxial tests. Based on the above reference book, the experiments whose target loading velocity and target maximum axial strain of the tests were respectively 0.1mm per minute and 15 percents were carried out.

3. TEST RESULT AND CONSIDERATIONS OF GDBP

3.1 Cyclic triaxial tests

Relations between axial strain and equivalent Young's modulus and hysteretic damping ratios of test pieces of (A) and (C) are shown in Figure 3.1(a). These of test pieces of (B) and (D) are shown in Figure 3.1(b). In both figures, strain dependency of equivalent Young's modulus or hysteretic damping ratios of Toyoura sand also displayed. Obviously, large values of the hysteretic damping ratios, approximately 15 percents to 22 percents, of each test piece can be seen without strain dependency. In case of Toyoura sand, these values of the hysteretic damping ratios can be obtained when the strain level becomes 0.001 or more that is the large strain level. This tendency has been also observed in the previous papers (Fujikawa *et al.*, 2011). The large values of the hysteretic damping ratios can be relatively obtained in case that asphalt emulsion (EA) is used as a binder and recycled fine powder (RF) is used as an admixture. Strain dependency of equivalent Young's modulus of the test pieces that used asphalt emulsion is less than those of Toyoura sand. In comparison with ratio of equivalent Young's modulus (decreasing rate of rigidity) at strain levels of 0.0001 and 0.001, the decreasing rates of rigidity for test pieces of (A) to (D) are approximately 9 to 20 percents, and the decreasing rate of rigidity for Toyoura sand is approximately 42 percents. Therefore, it is found that difference in both is quite large.

Focusing on the equivalent Young's modulus of test pieces of (B) and (D), these values are larger than that of Toyoura sand. Compounding ratios of WC of test pieces of (B) and (D) are smaller than those of (A) and (C), and test pieces of (B) and (D) include RF or BS more than these of (A) and (C). Hence, it is judged that RF or BS is the admixture that can obtain high equivalent Young's modulus.

3.2 Triaxial compression tests

The relation between differential stress and axial strain of each test piece is displayed in Figure 3.2. As a comparison, the relation of Fujinomori clay is also shown. As this result is obtained from a hollow cylindrical torsional shear test, the relation of the clay is calculated in case of Poisson's ratio = 0.5. At a certain strain, the differential stress curve of the clay shows the obvious peak value that is in the failure condition. On the other hand, the differential stress curve of each test piece does not have the specific peak value despite exceedance of 15 percents axial strain. It is observed that behaviors of the relations between differential stress and axial strain of test pieces of (A) and (C) versus (B) and (D) are different. This difference seems to be caused by effect of contained WC. When test pieces of (A) and (C) that contain a high proportion of WC are subjected to large axial deformations, they show an elastic behavior due to the close contact of each WC that has the compressive performance. In order to confirm further characteristics of each test piece that did not demonstrate any clear damage after triaxial compression tests, degrees of recovery of test pieces during one week were investigated. During the triaxial compression tests, test pieces were shrank up to 85 percents of the initial length of test pieces, but test pieces of (A) to (D) were recovered up to 93.4%, 89.3%, 91.6% and 89.5%,

respectively. Therefore, it is found that test pieces that contain high compounding ratio of WC can be recovered drastically.

Comparison of results between triaxial compression test and uniaxial compression test for specimen of (A) is illustrated in Figure 3.3. This comparison has presented the difference that GDBP is installed on the ground level or GDBP is embedded in soil at 5m depth. When axial strain is 15 percents, the differential stress of triaxial compression test is three times larger than that of uniaxial compression test. It is confirmed that the more GDBP is subjected to the confined pressure, the more rigidity of GDBP is increased.
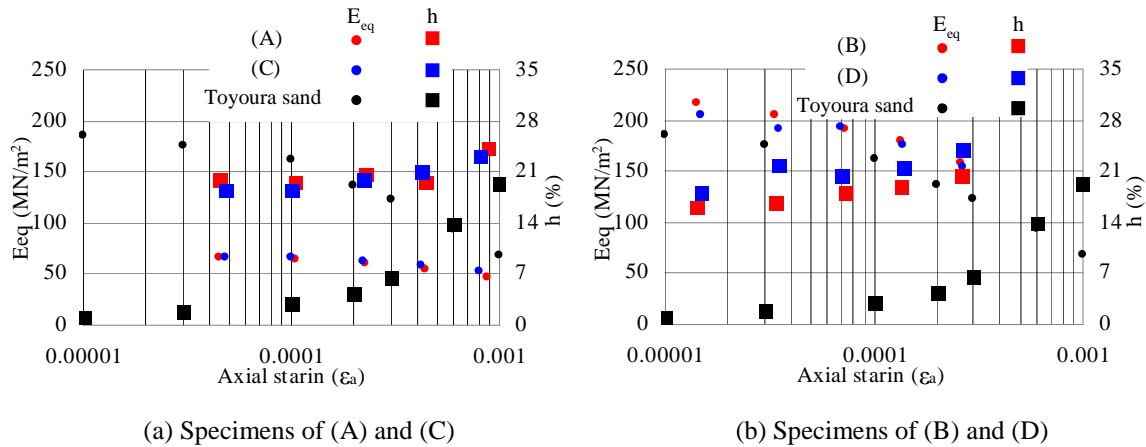

(a) Specimens of (A) and (C) (b) Specimens of (B) and (D)

Figure 3.1. Strain dependency of equivalent Young's modulus E_{eq} and hysteretic damping ratios h
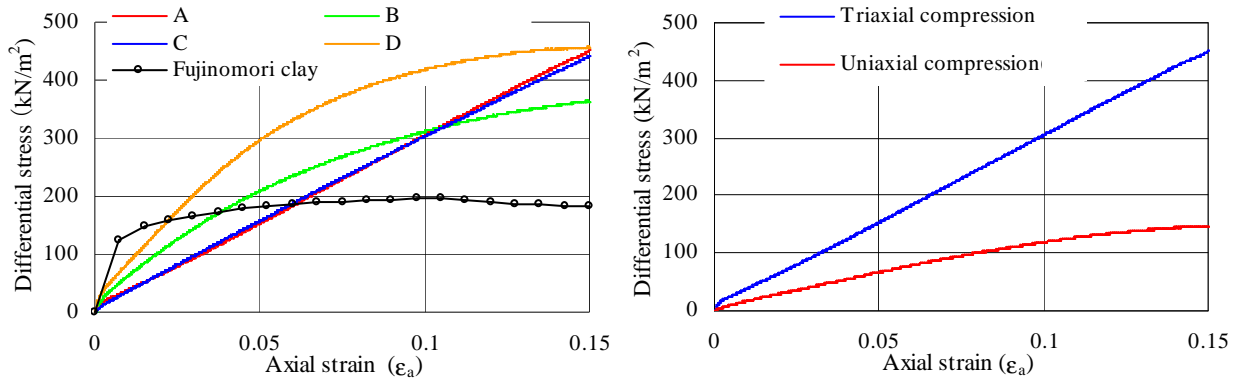

Figure 3.2. Relation between differential stress and axial strain

Figure 3.3. Comparison of results between triaxial and uniaxial compression tests for test piece of (A)

4. PRELIMINARY SEISMIC CALCUALTIONS OF BUILDING TAKING GDBP INTO ACCOUNT

4.1 Building and soil models

A mid-rise building is adopted for a model in the preliminary seismic analyses. Number of floors is six including roof floor and the basemat is embedded in soil. Dimension of the plan view of the building is square (25m x 25m) and each floor height is 3.5m. An embedded depth of the basemat is D = 5m. In these analyses, the basemat is assumed to be the rigid body. Superstructure of the building is modelled with concentrated masses and beam elements that are taken into bending and shear deformations account. The basemat, soil, GDBP and the high rigidity damping material (HRDM) are modelled using the 3-dimensional axial symmetry FE models, where HRDM is a composite of crushed stones,

waste tire chips and asphalt. By installing HRDM adjacently or underneath embedded foundations, it has been confirmed that HRDM make an important role of contribution for increase of static soil stiffnesses and damping coefficient of rocking in low frequency range. Analysis model is shown in Figure 4.1 and properties of the superstructure are described in Table 4.1 (Shimomura *et al.*, 2005).

Surface layer soil where the basemat is embedded is a uniform soil and its shear velocity and height are 100m/s and 10m, respectively. The surface layer soil is sustained by the supporting layer soil that is a half-space layer. Its shear velocity is 200m/s. An equivalent radius of the basemat is R=14.015m and axial symmetry FE model of the basemat is divided by two elements vertically. Heights of the upper portion and the lower portion are respectively (1/3)*D and (2/3)*D, as shown in Figure 4.2. Shear velocity, unit weight, Poisson's ratio and damping constant of each surface layer soil, supporting layer soil, GDBP and HRDM are displayed in Table 4.2. Material properties of GDBP and HRDM are estimated by results of the material tests.
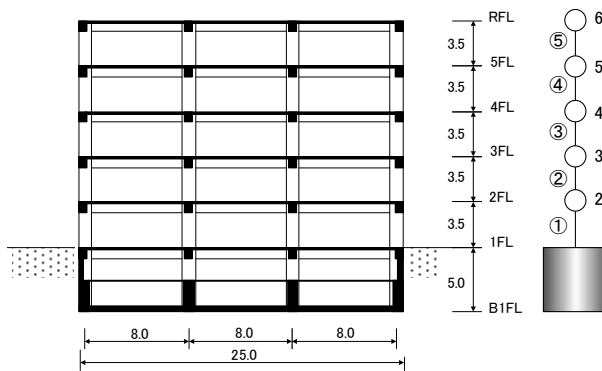

Figure 4.1. Target building and analysis model (superstructure including basemat)
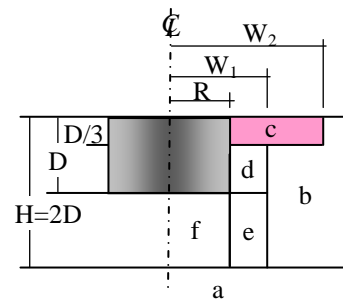

Figure 4.2. Analysis model (basemat and surrounding soil)

Table 4.1. Properties of superstructure

Node	Element	Height (m)	Mass (ton)	Shearing section area (m^2)	Moment of inertia (m^4)
6		22.5	890		
	⑤			0.3394	1280
5		19.0	890		
	④			0.3394	1280
4		15.5	890		
	③			0.3394	1280
3		12.0	890		
	②			0.384	1280
2		8.5	890		
	①			0.384	1280
Basemat			2920		

Table 4.2. Properties of soil and other materials

		Vs (m/s)	ρ (ton/m^3)	ν (Poisson's ratio)	h (damping ratio)
I	Supported soil	200	1.8	0.45	0.02
II	Surface layered soil	100	1.6	0.45	0.02
III	GDBP	150	1.2	0.35	0.20
IV	HRDM	200	1.7	0.35	0.20

Table 4.3. Analysis cases (soil and foundation)

Case	a	b	c	d	e	f
A	I	II	II	II	II	II
B	I	II	III	IV	II	II
C	I	II	III	IV	II	IV
D	I	II	III	IV	IV	IV

4.2 Calculation cases

Taking account of the planting capability of GDBP and effective utilization of GDBP for parking lots, GDBP is assumed to be applied to ground level. Based on the characteristic of HRDM already obtained, HRDM is also assumed to be mounted in adjacent lower portion of the embedded basemat or underneath the basemat.

Calculation cases considered in these analyses are shown in Table 4.3. 'Case A' is a basic model that has no soil improvement and comprises the surface layer soil and the supporting layer soil. In 'Case B', GDBP is applied to zone 'c' that is the adjacent upper portion of the embedded basemat in Figure 6. Height of zone 'c' is (1/3)*D and its width from the centerline of the basemat is $W_2 = 2*R$, where R is the equivalent radius of the basemat. HRDM is installed in zone 'd' which is underneath zone 'c'. Height and width of zone 'd' are (2/3)*D and $W_1 = (5/4)*R$, respectively. The width is a distance from the centerline of the basemat to edge of the zone 'd'. 'Case C' is modelled with a small modification of 'Case B'. The property of zone 'f' that is underneath the basemat is replaced the surface layer soil by HRDM. Height and width of zone 'f' are respectively D and R. 'Case D' is almost the same as 'Case C' except that the property of zone 'e' that is underneath zone 'd' is HRDM instead of the surface layer soil. Height of zone 'e' is D and its width from the centerline of the basemat is $W_1 = (5/4)*R$.

4.3 Horizontal and rocking impedance functions and equivalent damping constants

Horizontal and rocking components of impedance functions for each Case are calculated and based on these impedance functions, corresponding equivalent damping constants are also estimated. Comparisons of real and imaginary parts of the impedance functions for horizontal and rocking components in each Case are shown in Figures 4.3 and 4.4. Figure 4.5 illustrates the equivalent damping constants of horizontal and rocking components estimated from the impedance functions. X-axis of each figure means dimensionless frequency of $a_0 = \omega b/V_s$, where ω is the circular frequency, b is the half width of the square basemat and V_s is the shear velocity of the supporting layer soil. Y-axis of each impedance function means dimensionless stiffness of the ratio of each impedance function to the multiplications of b and G that is the shear modulus of rigidity calculated by V_s of the shear velocity of the supporting layer soil. The corresponding equivalent damping constants estimated from the impedance functions are calculated by the following formula:

$$h = \sin(\frac{1}{2}\tan^{-1}\frac{K'}{K}) \tag{4.1}$$

where K, K' are the real and imaginary parts of impedance functions.

Since the static stiffness depends on the shear velocity of the soil underneath or laterally the embedded basemat, the static stiffnesses of 'Case C' and 'Case D' are larger than those of 'Case A' and 'Case B'. This tendency can be seen in both horizontal and rocking impedances. Due to large effect which the bottom edge portions of the embedded basemat and the shear velocities of the surrounding soils have on the rocking stiffness, installation of HRDM in these portions of the embedded basemat provides larger differences of the rocking impedance than horizontal one. Focusing on the corresponding equivalent damping constants for rocking component, it is found that the corresponding equivalent damping constants for the rocking components among 'Case B', 'Case C' and 'Case D' prior to the cut-off frequency are larger than 'Case A', due to installation of HRDM underneath and/or along the side of the embedded basemat. In comparison of functions of the corresponding equivalent damping constants of the horizontal and rocking components, the contribution of installation of HRDM in the zone 'e' of 'Case D' is smaller than other Cases and the functions of the horizontal and rocking equivalent damping constants of 'Case D' are close to those functions of 'Case A' over $a_0 = 1.5$ and 2.0, respectively. It is expected that installing HRDM around and underneath the embedded basemat will be able to decrease the response of buildings by rocking mode prior to $a_0 = 2.0$.

4.4 Seismic analysis response of building

Transfer functions of typical floor levels against the surface of the free field are illustrated in Figure 4.6. Compared to 'Case A', the predominant frequency of 'Case D' obviously moves to the higher frequency range and the peak value of the transfer function of 'Case D' decreases. It is found that HRDM underneath or around the embedded basemat can reduce the rocking motions of the building as expected in the previous section. The reduction ratios of the peak values of the transfer functions between 'Case D' and 'Case A' at each floor level are approximately 45% to 50%, respectively. Since location of 4FL becomes a node of the vibration, the peak of the second mode is not seen on the transfer functions.

(a) Real part　　　　　　　　(b) Imaginary part
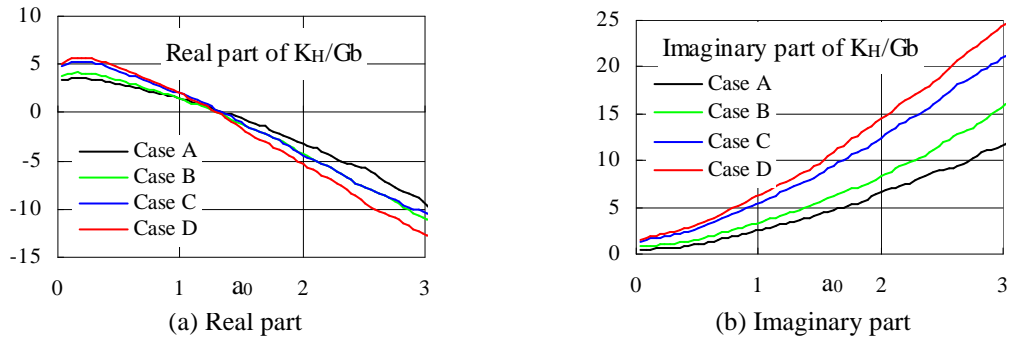
Figure 4.3. Impedance functions of horizontal component

(a) Real part　　　　　　　　(b) Imaginary part

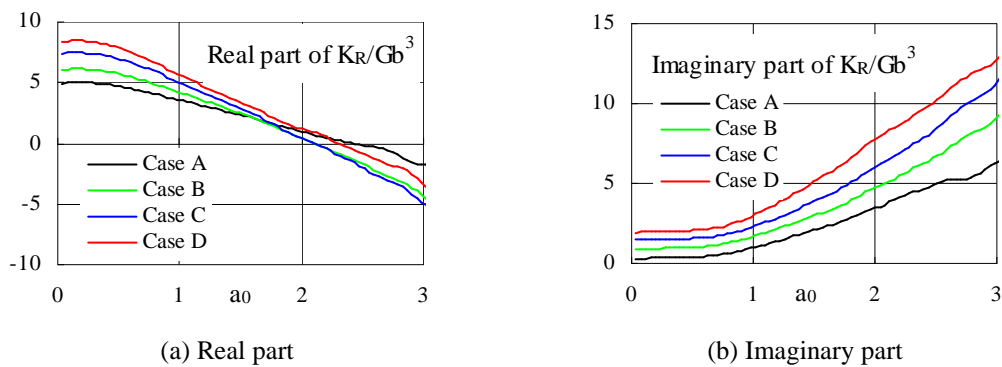**Figure 4.4.** Impedance functions of rocking component

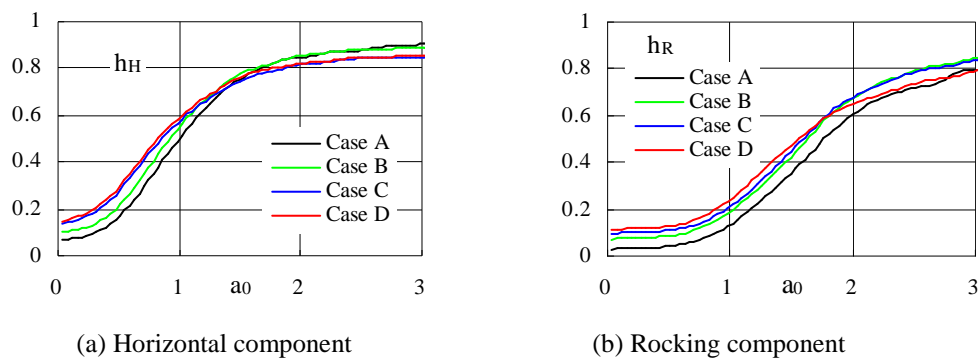(a) Horizontal component　　　　　　(b) Rocking component

Figure 4.5. Equivalent damping ratio of horizontal and rocking components
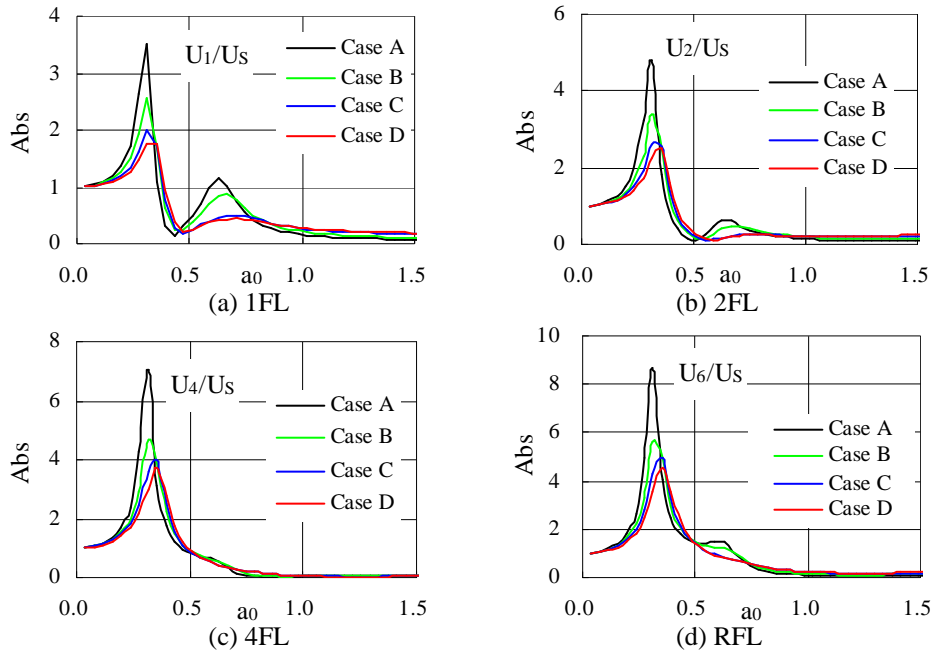
Figure 4.6. Transfer functions of typical floor levels against the surface of the free field

5. DYNAMIC CHARACTERISTICS OF RAISING MATERIAL BY ONE-DIMENSIONAL WAVE PROPOERGATION ANALYSES

5.1 Analyses models

Focusing on improvement of disaster areas that were sunken or flooded by the 2011 off the Pacific coast of Tohoku Earthquake, it is assumed that GDBP, HRDM and concrete rubble are adopted as the height increasing materials for the damaged soil areas of the afflicted district. Using the above materials as parameters of calculations, numerical analyses by the one-dimensional wave propagation theory are carried out. GDBP, HRDM and concrete rubble are adopted as the height increasing materials whose depth is 3m. Height of the surface layer soil and the supporting layer soil is 20m. It is assumed that 'TYPE 0' is the damaged soil layer by the tsunami and the earthquakes. 'TYPE 1' takes into account the height increasing layer that has the same property of the surface layer soil. In 'TYPE 2', GDBP is adopted as the material of the height increasing layer. 'TYPE 3' takes account of HRDM as the height increasing material. In 'TYPE 4', GDBP of 1m and HRDM of 2m are adopted for materials of the height increasing layer. In 'TYPE 5', concrete rubble that is not required radiation decontamination is utilized as the material of the height increasing layer. All soil model of the one-dimensional wave propagation analyses are shown in Figure 5.1. Materials adopted in these analyses are shown in Table 5.1.

5.1 Results of response analyses

Seismic response amplification ratios of top surface of soil deposits against twice the incident wave are displayed in Figure 5.2. Natural frequencies of the soil deposits which have the height increasing soil layers shift to low frequency range, and effects of the height increasing material layers can be seen in higher frequency range. Especially, 'TYPE 3' and 'TYPE 5' that take into account HRDM and concrete rubble as the height increasing materials show the effect of attenuation from low frequency range. On the other hand, despite of same value of the damping constant considered, response amplification ratios of 'TYPE 2' and 'TYPE 4' that use GDBP as the height increasing material are larger than those of 'TYPE 3' and 'TYPE 5'. Because the impedance ratios of GDBP against the surface layer soil is smaller than these of HRDM against the surface layer soil, amplification ratios of

'TYPE 2' and 'TYPE 4' are larger than these of 'TYPE 3' and 'TYPE 5'. Actually, since GDBP contains wood-chips, the unit weight of GDBP becomes small. In order to mitigate amplification ratio of the height increasing soil layer, the impedance ratio of the height increasing material should be greater than that of the surface soil layer.
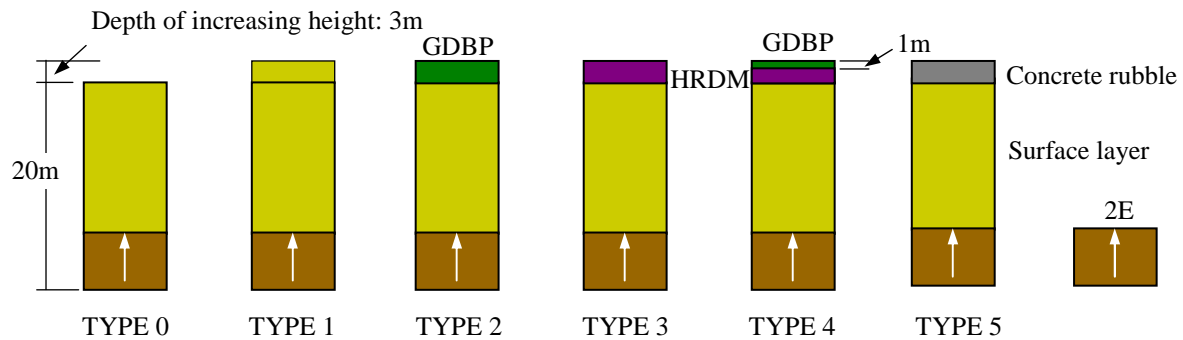

Figure 5.1. Analysis models for one-dimensional wave propagation analysis

Table 5.1. Properties of soil and other materials

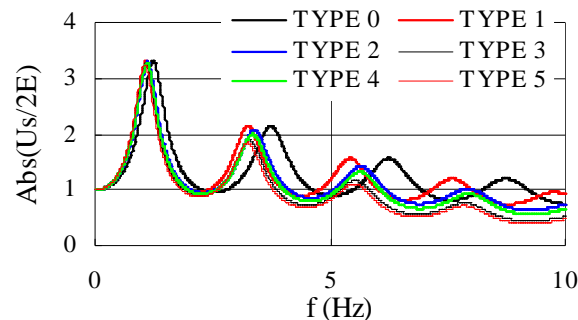|	ρ (ton/m^3)	Vs(m/s)	h
Surface layer	1.7	100	0.05
Bedrock	1.9	400	0.01
GDBP	1.2	150	0.20
HRDM	1.4	250	0.20
Concrete rubble	1.9	250	0.05

Figure 5.2. Transfer functions (U$_S$/2E) of each TYPE

6. CONCLUSIONS

Laboratory tests for a new soil material, that is, GDBP that uses industrial wastes and construction by-products were carried out to grasp its dynamic characteristics. The following features were obtained.
1) If asphalt and microgranule will be combined with the proper ratio as a binder, GDBP can obtain high attenuation performance regardless of kinds of admixtures.
2) Depending on kinds of admixtures, values of the Young's modulus of GDBP are varied dramatically and their range become over 20 times.

Based on preliminary seismic response analyses using HRDM and GDBP as soil improvement materials, the following results were summarized.
1) Installation of HRDM in the bottom edge portions of the embedded basemat provides reduction of rocking motion of the basemat.
2) Reduction ratio of the peak values of the transfer functions of the building (at the roof level) that

takes account of HRDM and GDBP underneath and around the embedded basemat is about 50%.

Using the height increasing soil model taking into account the post-disaster restoration, the one-dimensional wave propagation analyses were conducted. Summary of results are shown below.
1) It is found that seismic response amplification ratios of the transfer functions of the building depend on Young's modulus and unit weight of the height increasing soil materials. Especially, the impedance ratio of the soil deposit affects the seismic response amplification ratios larger than the soil damping.

In accordance with soil deposits to be improved, variety of admixtures for GDBP should be considered. In future laboratory tests, kinds of rubble of the 2011 off the Pacific coast of Tohoku Earthquake and tsunamis that will mix with GDBP have to be investigated. Additional seismic analyses taking account of applicability of the height increasing soil materials for the damaged soil area will be also performed.

REFERENCES

Fujikawa T., Shimomura Y., Sako N. and Kawamura M. (2011), Cyclic Deformation and Triaxial Compression Properties of New Geomaterial Damping Blocks, *Summary of Technical Papers of Annual Meeting of Architectural Institute of Japan*, **B1**, 557-558 (in Japanese).

Hirota, M., Ishimura, K., Suzuki, Y., Miura, K., Nagano, M. and Kiyota, A. (1993), Development of Foundation Work for Reduction of Earthquake Response - Part1 Analytical Examinations and Material Tests. *Journal of Structural and Construction Engineering*, AIJ, **No. 448**, 37-46 (in Japanese).

Japanese Geotechnical Society (2009), Japanese Standards for Geotechnical and Geoenvironmental Laboratory Testing Methods – Standards and Explanations, 579-583, 751-759 (in Japanese).

Sako N., Ikeda Y., Shimomura Y. and Kawamura M. (2010), Development of A New Geomaterial for Base Isolation Foundations, *Fifth International Conference on Recent Advances in Geotechnical Earthquake Engineering and Soil Dynamics*, Paper No.1.29a (CD).

Shimomura Y., Ikeda Y., Kawamura M. Sako N. and Ishimaru S. (2008), Proposal of New Foundation Construction Works with High Damping and Mitigation Performance- Part 2 Earthquake Observation of Blocks and Seismic Response Prediction of Full-scaled Foundations, *Proceedings of the 14th World Conference on Earthquake Engineering*, Paper No.04-01-0017 (DVD).